LA-UR-93-2080

Los Alamos National Laboratory is operated by the University of California for the United States Department of Energy under contract W-7405-ENG-36

TITLE Mach Reflection of Spherical Detonation Waves

AUTHOR(S) Lawrence M. Hull, M-8

SUBMITTED TO Fourth International Detonation Symposium

DISCLAIMER

Los Alamos National Laboratory
Los Alamos, New Mexico 87545

MACH REFLECTION OF SPHERICAL DETONATION WAVES

L. M. Hull
Los Alamos National Laboratory
Los Alamos, NM 87544

When two detonation waves collide, the shape of the wave front at their intersection can be used to categorize the flow as regular or irregular reflection. In the case of regular reflection, the intersection of the waves forms a cusp. In the case of irregular reflection, the cusp is replaced by a leading shock locus that bridges the incident waves. Many workers have studied irregular or Mach reflection of detonation waves,[1-4] but most of their experimental work has focused on the interaction of plane detonation waves. Reflection of spherical detonation waves has received less attention. This study also differs from previous work in that the focus is to measure the relationship between the detonation velocity and the local wave curvature for irregular reflection of spherical detonation waves. Two explosives with different detonation properties, PBX 9501 and PBX 9502, are compared.

INTRODUCTION

Recent work in this country and in the UK indicates that divergent detonation wave propagation can be described in terms of a relationship between the local wave curvature and the local normal detonation velocity (see Refs. 5-7). In the U.S.A., the theory is called Detonation Shock Dynamics (DSD). The application of DSD to convergent waves has a less solid theoretical foundation because the flow behind the convergent wave is subsonic and can thus be influenced by disturbances propagated forward to the wave front. Whitham's[8] method for treating shock diffraction in gas dynamics suffers from the same difficulty; nevertheless, it has been successful. The results presented here, along with those of Bdzil and Davis,[9] show that the detonation velocity is related to the local wave curvature in a continuous manner from convergent to divergent configurations. Thus it may be possible to apply wave tracking methods, based on DSD, to arbitrary convergent and divergent geometries, with success similar to that enjoyed by Whitham's method.

When two divergent spherical detonation waves collide, regular reflection is first observed and, subsequently, irregular reflection develops. The Mach stem is the bridge that develops between the spheres. Hereon, any irregular reflection is called a Mach reflection.) The saddle surface generated by the collision (Figure 1) is a surface of revolution that is truncated because of the finite dimensions of the explosive. Therefore, the intersection of the surface with a plane results in a record of the temporal evolution of the surface. To describe the entire surface generated when two divergent spherical waves collide, all the usual parameters that describe wave reflection must be measured or calculated, as well as the parameters that describe the expanding spherical waves. Experimental wave arrival time data are modeled with analytic functions to describe the wave shape and propagation for both the convergent and divergent waves. We also use metal plate acceleration experiments and assumed equations of state to provide independent measurements of the pressure in the Mach reflection region.

A surface has two principal radii of curvature. We have chosen the mean curvature as the descriptive parameter. The sign of the mean curvature κ is chosen so that a divergent wave has positive curvature. The mean curvature of the saddle point (Mach stem) is negative and approaches zero as the spheres expand and the Mach stem grows. The data analysis technique assumes that the $D(\kappa)$ relationship is linear, primarily because this is the simplest form. The convergent wave results are only slightly dependent on this assumption. The linear relationship can be written as

$$D = D_0(1 - a\kappa), \qquad (1)$$

where D is the local detonation velocity, D_0 is the C-J detonation velocity, a is a coefficient dependent on the explosive, and κ is the mean curvature of the detonation wave. For a spherical wave, $D = dh/dt$, so substitution of Equation (1) and integration with respect to time gives

$$D_0 t = r_0 - r + a \ln\left(\frac{r_0 - a}{r - a}\right). \qquad (2)$$

Equation 1 applies to both convergent and divergent flow, but Equation 2 applies only to the spherically expanding waves.

of curvature r_m, so r dominates the estimated mean Mach stem curvature from the data. On the other hand, the velocity of the Mach stem is the rate of increase of r_m. Therefore, accurate measurement of both r_m and r_s is necessary to determine the D-κ relationship for the convergent region.

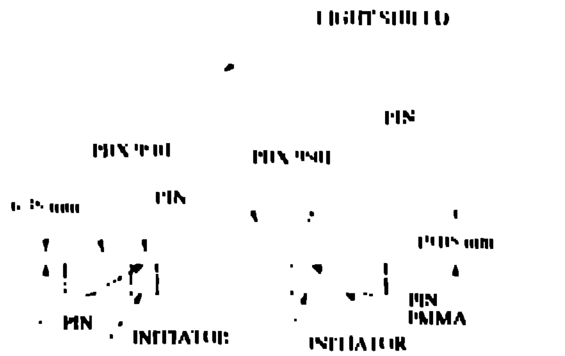

FIGURE 2. DIVERGENT WAVE CHARACTERIZATION EXPERIMENT

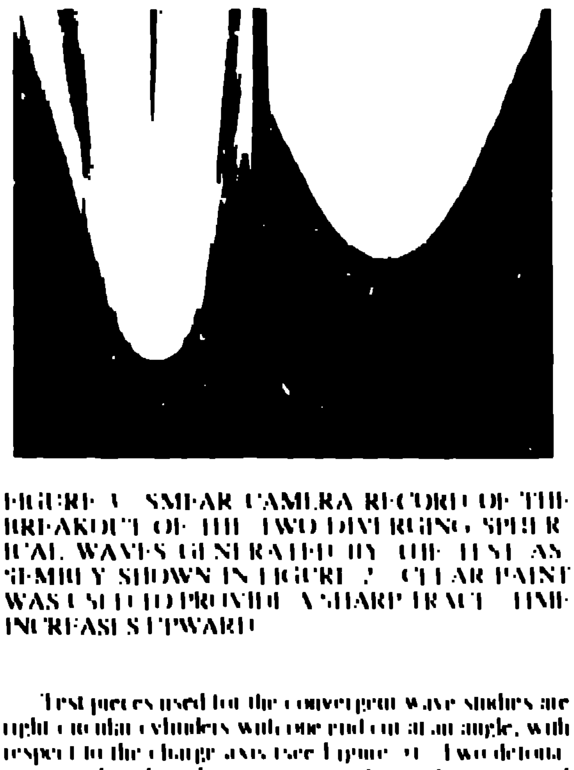

FIGURE 3. SMEAR CAMERA RECORD OF THE BREAKOUT OF THE TWO DIVERGING SPHERICAL WAVES GENERATED BY THE TEST ASSEMBLY SHOWN IN FIGURE 2. CLEAR PAINT WAS USED TO PROVIDE A SHARP TRACE. TIME INCREASES UPWARD.

FIGURE 1. MACH REFLECTION OF SPHERICAL DETONATION WAVES. DETONATIONS WERE INITIATED AT (0,±50,0) AND WAVE FRONT ARRIVAL RECORDED BY A SMEAR CAMERA. THE RECORDS WERE ANALYZED AND INTERPOLATED TO OBTAIN AN APPROXIMATION OF THE SHAPE OF THE COMPLETE SURFACE.

EXPERIMENTAL

The divergent wave detonation velocity curvature relationship for PBX 9501 was determined with the experiment shown schematically in Figure 2. Two detonator booster systems were placed so as to initiate the explosive under two thicknesses of the test explosive. The arrival time of the detonation wave at the observation surface over the center of each detonator was recorded through a single slit with the smear camera (Figure 3). Camera data corresponding to each wave were modeled as a sphere located at some arbitrary origin, the sphere expanded at a constant velocity only for the duration of the breakout at the free surface. Position time data from the region directly over the detonators were fit to the model equation to determine the radius of each wave. When the measured radii and time differences are used to solve Equation (2) with D_{CJ} = 8.802 mm/μs, ... [illegible] mm. Then Equation (1) gives the corresponding values of κ so that we have two D(κ) points.

To determine the variation of the detonation velocity with the local mean surface curvature for convergent detonations, the Mach reflections of two propagating spherical detonation waves are measured. The mean curvature of the saddle surface, and thus the Mach stem, is the mean of the two principal curvatures. These principal curvatures are the inverse of the radius of curvature of the intersection of the saddle with the x-y plane (r_m), and the inverse of the radius of curvature of the intersection of the saddle with the y-z plane at x = 0 (see Figure 1) ... [illegible]

Test pieces used for the convergent wave studies are right circular cylinders with one end cut at an angle, with respect to the charge axis (see Figure 4). Two detonators are placed on the x axis at x = ±y and are initiated simultaneously. The arrival of the detonation wave at the angled observation surface is recorded through 11 slits with a smear camera. Slits are arranged parallel to the x axis with the center slit at x = 0. A typical camera record is shown in Figure 6. The curved Mach stem can be clearly seen at the intersection of the two spheres.

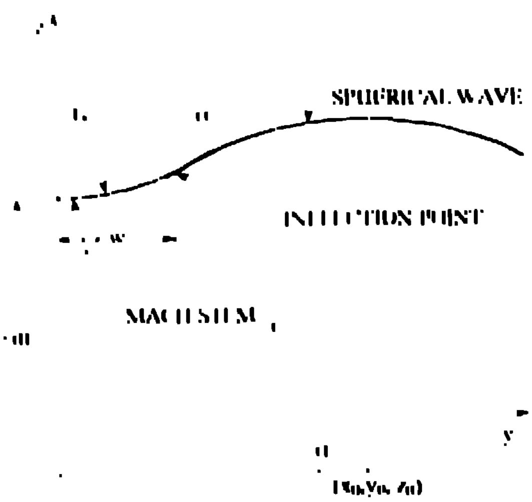

FIGURE 4. THE GEOMETRY OF THE MACH REFLECTION OF SPHERICAL WAVES

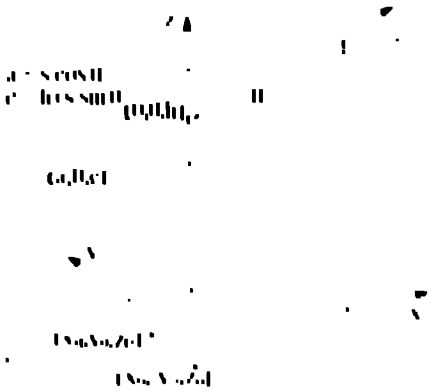

FIGURE 5. SHOT GEOMETRY FOR MACH STEM EXPERIMENTS

The arrival time data, well away from the Mach stem, are fit to the equation of a sphere centered at (x_0, y_0, z_0) and expanding as given by Equations 1 and 2. At each slit, the values of x [illegible] and z [illegible] are known from the geometry. Therefore, the model function for the expanding wave becomes

$$(x - x_0)^2 + (y - y_0)^2 + (z - z_0)^2 = r^2, \qquad (3)$$

the data set is [illegible], and the parameters determined by the fit are x_0, y_0, z_0, and t_0. The [illegible] value in Equation (1) is taken to be $|z_0|$. The use of Equations (1) and (2), rather than a sphere expanding at the CJ velocity, results in a small correction because the radius of the sphere is large, compared with [illegible]. A fixed value of [illegible] was used for PBX [illegible] and a value of [illegible] was used for PBX [illegible]. An example of the result of the curve fit is given in Figure 7. The value of r_{m} for each slit is given by

$$(r_m)^2 = (x - x_0)^2 + (z - z_0)^2. \qquad (4)$$

The corresponding arrival time of the Mach stem at y = 0 is known from the data; differentiation of this (r_m, t) data gives the normal velocity of the Mach stem, $D = dr_m/dt$.

FIGURE 6. A MULTISLIT SMEAR CAMERA RECORD OF SPHERICAL DETONATION WAVE INTERACTION IN PBX 9501. TIME INCREASES UPWARD

The arrival time data in the saddle region defines the shape of the Mach stem and allows the estimation of the Mach stem radius of curvature [illegible]. Mach stem data are fit to the equation of a circle lying in the [illegible] plane ([illegible] is the normal direction of the Mach stem). The center of the circle is moving in the [illegible] direction at the velocity for that particular slit, and the radius of the circle is [illegible]. Therefore, the model equation we use to determine [illegible] is

$$[illegible]$$

where data to be fit are [illegible] and the parameters are [illegible], and [illegible]. Note that this is a different [illegible] than in the previous discussion. The result of this curve fitting procedure for the [illegible] is given in Figure 8 [illegible]

was used to select the number of data points to be included in the curve fit. The r_s data for PBX 9501 are in the approximate interval $4 < r_s < 27$ mm and for PBX 9502 in the approximate interval $9 < r_s < 34$ mm. Thus we are approaching the region where the radius of curvature of the wave front is comparable to the reaction zone thickness (the distance from the leading shock to the sonic locus), a region of questionable applicability of DSD. The theoretical basis of DSD and the applicability of Equation (1) are dependent on the condition that the inverse of the wave curvature is much greater than the reaction zone thickness.

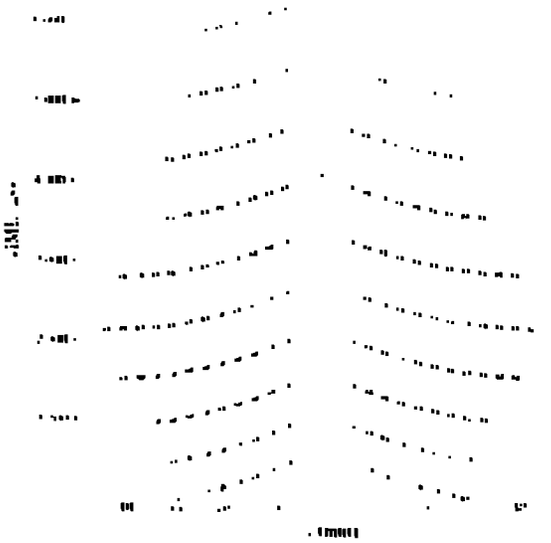

FIGURE 7. DATA AND CURVE FIT USED TO FIND THE ORIGIN OF THE SPHERICALLY EXPANDING PART OF THE DETONATION WAVE FOR THE RECORD SHOWN IN FIGURE 6

The mean curvature, $\kappa = 1/2\,(1/r_m - 1/r_s)$, can now be calculated and the $D(\kappa)$ relationship plotted (see Figure 9). Results for PBX 9501 indicate that, to within a good approximation over the measured range, the $D(\kappa)$ relationship is continuous and linear for both $\kappa > 0$ and $\kappa < 0$. The $D(\kappa)$ relationship for PBX 9502 is linear in the convergent region evaluated here. Slope is for PBX 9502 is large, in comparison with that of PBX 9501. The PBX 9502 $D(\kappa)$ relationship for $\kappa < 0$ is nonlinear.[9] The data from Holzl and Davis's study[9] and this study patch together the $D(\kappa)$ relationship appears to be continuous in both slope and magnitude across $\kappa = 0$. These relations can now be used with a detonation front tracking routine (see Reference 10) to predict wave profiles for both convergent and divergent waves.

Properly defined, the Mach stem width is the transverse distance from the plane of symmetry to the position of the intersection of the incident detonation and the discontinuity reflected into the products. The position of the reflected discontinuity is not readily available from arrival time data. Therefore, we choose to assume that the transverse position of the intersection point of the leading wave front defines the stem width. Figure 10 shows the Mach stem width data as a function of position r_m. The estimated Mach stem width w completes the information necessary to calculate the interaction angle α from $r \cos \alpha = y_0 - w$ (see Figure 4). By this calculation, we show that the measurements are for interaction angles that vary from about 70° to 75° for both PBX 9501 and PBX 9502. Although we have made measurements over a limited range of interaction angle, the Mach stem dimensions detected are initially only slightly larger then the reaction zone thickness and they are observed until nearly plane wave conditions are achieved. Over the measured range, the growth rate of the Mach stem is approximately constant. From the linear fit shown in Figure 10, the growth angle for PBX 9501 is $\chi = 2.4°$ and for PBX 9502, $\chi = 7.4°$. Extrapolating the linear relationship to $w = 0$ allows the estimation of the critical angle (the value α_c, at which an irregular reflection first appears). For PBX 9501 $\alpha_c = 56°$, and for PBX 9502 $\alpha_c = 63°$. This extrapolation is expected to overestimate the critical angle because of the neglected variation of the growth rate of the stem.

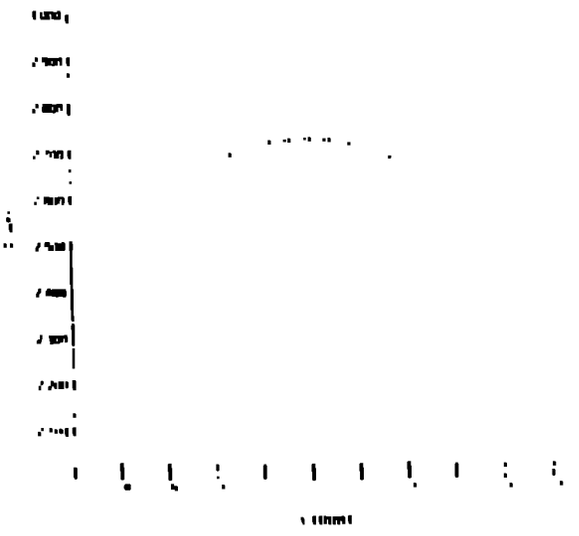

FIGURE 8. DATA AND CURVE FIT TO THE CENTER SLIT MACH STEM REGION OF THE RECORD SHOWN IN FIGURE 6. THE RADIUS VALUE OBTAINED IS 164 mm

In the reflectance gauge flash gap (RFG-FG) test, a 3 mm thick aluminum plate is placed on top of a right circular cylinder of explosive, along with a piece of Lucite® in which a gap is machined and polished.* The plate surface is illuminated with an argon lamp, and the slit of a smear camera is aligned parallel with the line defined by the detonations and the gap. When a shock wave arrives at the metal air interface, the diffuse reflectivity of

* Lucite is a registered trademark for acrylic resins, E. I. du Pont de Nemours & Co.

the surface is reduced. This is recorded by the smear camera as reduced exposure on the film. The metal plate arrives at the Lucite surface and causes the trapped air to flash, and the subsequent shock induced in Lucite causes the Lucite to become opaque. This is recorded on the smear camera as a thin line of bright light. From the known gap depth and time difference, we calculate the average free-surface velocity of the aluminum plate.

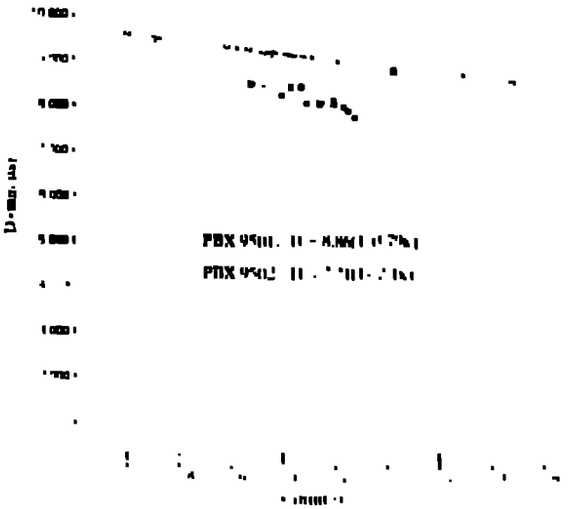

FIGURE 9 THE DETONATION VELOCITY CURVATURE RELATIONSHIP FOR PBX 9501 (THE OPEN CIRCLES) AND PBX 9502 (THE SOLID CIRCLES). THE BLACK SQUARE IS A PBX 9404 POINT TAKEN FROM REFERENCE 14

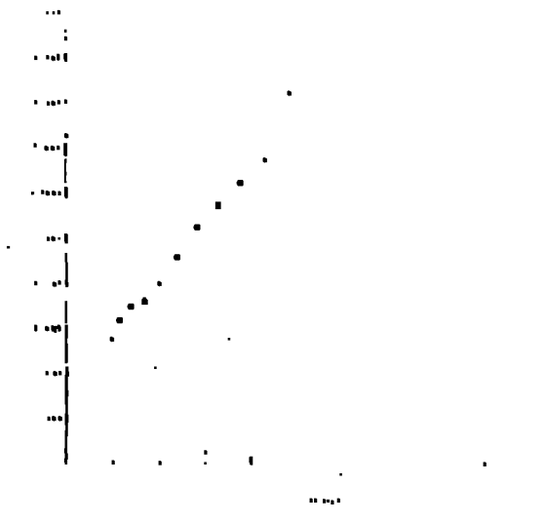

FIGURE 10 THE MACH STEM WIDTH AS A FUNCTION OF DETONATION THE SLOPE OF THE LINE GIVES THE GROWTH ANGLE OF THE STEM

Figure 11 reproduces records obtained in reflectance change flash gap experiments. The absence of a cusp in the reflectance-change trace in Figure 11a indicates irregular or Mach reflection. The presence of a cusp in Figure 11b indicates regular reflection. Dips toward earlier time at the center line of the flash trace imply that greater velocity is induced in the plate by higher pressure in the interaction region. We assumed that the particle velocity of the aluminum is one-half the measured free-surface velocity and that the free surface velocity vector bisects the original surface normal and the shock front normal. To find the detonation wave pressure, the pressure and particle velocity of the explosive products and aluminum are shock matched (assuming the products follow the JWL equation of state). A curve-fitting procedure similar to the multistreak technique outlined above is used to find the interaction angle α.

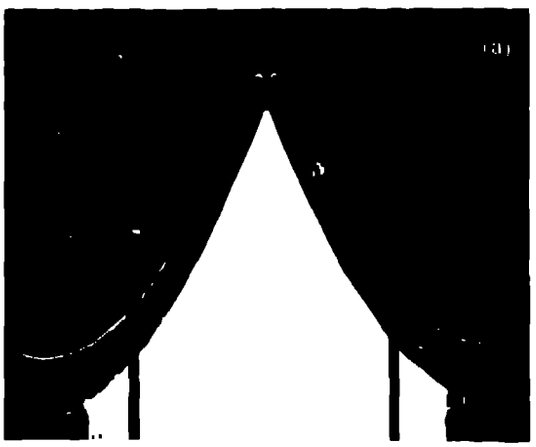

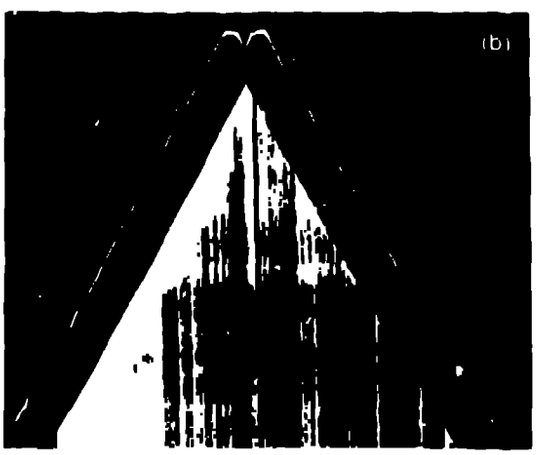

FIGURE 11 RECORD OBTAINED FROM REFLECTANCE CHANGE FLASH GAP EXPERIMENTS IN PBX 9501. (a) IRREGULAR OR MACH REFLECTION. (b) REGULAR REFLECTION. TIME INCREASES DOWNWARD

ANALYSIS

The data are best discussed in the context of an analysis. The most basic analysis is to approximate the flow as the intersection of two plane waves that are tangents to the spheres. Flow is separated into regions by the detonation and shock waves, the flow in each region is assumed to be one-dimensional, and all waves are assumed to follow the appropriate jump conditions. This is the classical shock polar theory of gas dynamics, a tool found useful over the decades and still in use today.[11-13] The quasi-steady assumption now encompasses the effects of interaction angle variation with time.

Figure 12 represents the geometry of the classical Mach reflection analysis. The plane of symmetry of the colliding spherical waves is represented as a perfectly rigid wall. Figure 12 shows the Mach stem as a straight line. However, other assumptions can be made about the shape of the Mach stem and the resulting trajectory of the triple point. The triple point follows a path that makes an angle χ with the wall. In a stem that grows, the velocity of the point P is given by

$$\dot{V}_p = D_1 \csc(\alpha - \chi)\cos\chi\,\hat{i} + D_1 \csc(\alpha - \chi)\sin\chi\,\hat{j}. \quad (6)$$

In general, χ is variable and the path can have curvature. Additionally, for interacting spheres, α is variable.

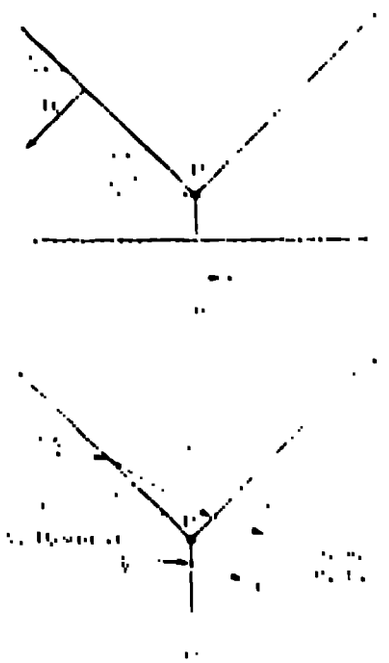

FIGURE 12. MACH REFLECTION OF A PLANE WAVE FROM A RIGID WALL (AT A LABORATORY COORDINATES; (B) COORDINATES ATTACHED TO P

The system of equations is closed by requiring the flow velocity in regions 3 and 4 to be parallel and the pressures in regions 3 and 4 to be equal. Regions 3 and 4 are separated by a contact discontinuity (slip stream); the velocities differ, but the pressures are equal.

Our experimental observation is that the Mach stems are curved, they grow, and they are normal to the plane of symmetry. Thus the flow is at least two-dimensional in the region behind the stem and the "triple point" may degenerate into a region of interaction between the incident detonation and the reflected disturbance. In general, the rate of growth of the Mach stem will not be constant. On the other hand, our data (Figure 10) show that the growth rate is fairly constant over the interval observed. Because the observed stems are curved, we also expect that the straight-stem assumption will overpredict the growth rate. Therefore, we compare our pressure data to the results of the shock polar analysis using both the straight-stem assumption and the constant growth rate (measured) assumption. From Figure 12, if the growth rate and interaction angle are both specified, the pressure behind the stem is easily calculated from the jump conditions.

The explosive is assumed to follow the JWL equation of state. Figure 13 shows the pressure produced by the wave interaction for both regular and Mach reflection as a function of interaction angle. For low values of α, regular reflection occurs. As the critical angle α_c is approached, the pressure increases. When Mach reflection first appears, the pressure jumps discontinuously to very high values. As α becomes larger in the Mach reflection regime, the pressure decreases and eventually approaches the CJ value. Mach stems near the critical angle would be the size of the reaction zone or smaller. Thus the classical theory, which assumes a jump from the initial state to the fully detonated state, may not apply.

For regular reflection ($\chi = 0$, $\alpha < \alpha_c$), the pressure calculated from the theory and the data from the RCTG experiments agree reasonably well. For Mach reflection, pressure calculated from the theory using the straight stem assumption is significantly greater than the data from the RCTG experiments. Use of the measured value of χ, which forces the measured Mach stem velocity, brings the calculation into agreement with the pressure measured in the RCTG experiments. The values of χ calculated from the straight stem assumption are considerably larger than the measured values. This results in overprediction of the phase velocity along the plane of symmetry, and so also overpredicts the pressure behind the stem.

CONCLUSION

The data show that, over the measured interval, the detonation velocity is a continuous function of curvature for convergent flow, in spite of the presence of subsonic flow behind the Mach stem. The (Dκ) relationships provided by this study combined with that of Reference 9 allow the calculation of convergent and divergent detonation wave propagation in PBX 9501 and PBX 9404.

using DSD wave trackers. Comparisons of such calculations with experiments are required to determine the extent of applicability of DSD to convergent detonation waves.

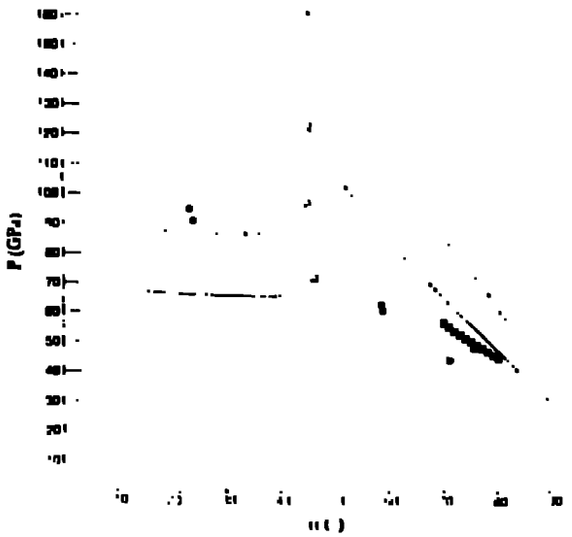

FIGURE 13. PRESSURE BEHIND THE REFLECTED WAVE AS A FUNCTION OF INTERACTION ANGLE. THE OPEN CIRCLES INDICATE PBX 9501 AND THE OPEN SQUARES INDICATE PBX 9502. THE BLACK SQUARES INDICATE THE PRESSURE CALCULATED WITH THE MEASURED GROWTH ANGLE AND THE BLACK DOTS INDICATE THE PRESSURE MEASURED WITH THE RCTG TECHNIQUE, BOTH FOR PBX 9501

The classical shock polar theory fails to accurately replicate the parameters of the flow when the straight Mach stem assumption was used, but use of the measured stem growth rate brings the theory into agreement with the experiment. Therefore, the analytic treatment requires proper handling of the curved-stem growth rate dynamics. Equation (1) used with Whitham's method suggests a nonlinear diffusive Mach stem growth process.[7] For application to spherical wave interactions, the process must be convoluted with the time-dependent boundary condition introduced by the spherically expanding wave. This modeling approach seems valid and is a current topic of our research.

Both the classical shock polar theory and the use of DSD wave trackers are expected to be applicable when the features such as the Mach stem width and the inverse of the surface curvature are relatively large, compared with the reaction zone thickness. The study of the flow where the features of interest are smaller than the reaction zone thickness remains unprobed by this study. Recent computer simulations[8] by Stewart suggest that reflection configurations familiar from gas dynamics may occur entirely within the reaction zone or span across the reaction zone.

REFERENCES

1. Gardner, S. D., and Wackerle, J., "Interactions of Detonation Waves in Condensed Explosives," *Proceedings of the Fourth Symposium (International) on Detonation*, October 1965, pp. 154-155.

2. Lambourn, B. D., and Wright, P. W., "Mach Interaction of Two Plane Detonation Waves," *Proceedings of the Fourth Symposium (International) on Detonation*, October 1965, pp. 142-152.

3. J. P. Argous, C. Peyre, and J. Thouvenin, "Observation and Study of the Conditions for Formation of Mach Detonation Waves," *Proceedings of the Fourth Symposium (International) on Detonation*, October 1965, pp. 135-141.

4. Mader, C. L., "Detonation Wave Interactions," *Proceedings of the Seventh Symposium (International) on Detonation*, June 1981, pp. 669-677.

5. Stewart, D. S., and Bdzil, J. B., "The Shock Dynamics of Stable Multidimensional Detonation," in *Combustion and Flame*, 72, 311-323 (1988).

6. Bdzil, J. B., Fickett, W., and Stewart, D. S., "Detonation Shock Dynamics: A New Approach to Modeling Multi-dimensional Detonation Waves," *Proceedings of the Ninth Symposium (International) on Detonation*, August 1989, pp. 730-742.

7. Lambourn, B. D. and Swift, D. C., "Application of Whitham's Shock Dynamics Theory to the Propagation of Divergent Detonation Waves," *Proceedings of the Ninth Symposium (International) on Detonation*, August 1989, pp. 784-797.

8. Whitham, G. B., **Linear and Nonlinear Waves**, John Wiley & Sons, New York, 1974.

9. Bdzil, J. B. "DSD Calibration for PBX 9502", *Proceedings of the Tenth Symposium (International) on Detonation*, July 1993.

10. Fickett, W. and Bdzil, J., "DSD Technology - A Detonation Reactive Huygens Code" Los Alamos National Laboratory report LA 12215 MS, (1992).

11. Courant, R. and Friedrichs, K. O., *Supersonic Flow and Shock Waves*, Interscience, New York, 1948.

12. Hornung, H., "Regular and Mach Reflection of Shock Waves," *Ann. Rev. Fluid Mech.* Vol. 18, No. 11, (1986) pp. 58.

13. Ben Dor, G. and Takayama, K., "The Phenomena of Shock Wave Reflection — A Review of Unsolved Problems and Future Research Needs," *Shock Waves* Vol. 2, 1992, pp. 211-223.

14. Campbell, A. W. and Engelke, Ray, "The Diameter Effect in High-Density Heterogeneous Explosives," *Proceedings of the Sixth Symposium (International) on Detonation*, August 1976, pp. 642-652.

15. Stewart, D. S. "CMHOG Calculations of a Reactive Wave Interaction" personal communication, 1993.